

# The SPICA Coronagraph Project

**L. Abe<sup>1</sup>, K. Enya<sup>2</sup>, S. Tanaka<sup>2</sup>, T. Nakagawa<sup>2</sup>, N. Murakami<sup>3</sup>, J. Nishikawa<sup>3</sup>,  
M. Tamura<sup>1</sup>, K. Fujita<sup>4</sup>, Y. Itoh<sup>4</sup>, H. Kataza<sup>2</sup>, O. Guyon<sup>5</sup>,  
and the Spica Working Group.**

<sup>1</sup>*Optical and Infrared Astronomy Division, National Astronomical Observatory of Japan, <sup>2</sup>Department of Infrared Astrophysics, Institute of Space and Astronautical Science, Japan Aerospace Exploration Agency,*

<sup>3</sup>*MIRA Project, National Astronomical Observatory of Japan, <sup>4</sup>Graduate School of Science and Technology, Kobe University, <sup>5</sup>Subaru Telescope*

## ABSTRACT

We present the latest results of our coronagraphic instrumentation study for the Japanese 3.5m SPICA telescope. Our aim was to validate some of the candidate concepts, amongst which the binary checkerboard mask (Kasdin et al. 2003). This solution benefits from theoretical intrinsic achromaticity, simplicity of its optical implementation which is a key issue since the SPICA telescope is designed to work at cryogenic (4.5K) temperatures. The huge drawback of this solution is its poor so-called inner working angle (IWA) and its overall transmission. This solution, although a clear compromise between performance and complexity, has proven to be a secured backup solution for the SPICA coronagraph.

## SPICA MISSION SUMMARY

The Space Infrared telescope for Cosmology and Astrophysics (SPICA) is the next generation mission for infrared astronomy led by Japan (Nakagawa et al. 2004). The SPICA telescope uses on-axis Ritchey-Chretien optics with a 3.5m diameter monolithic primary mirror. The whole telescope will be cooled to 4.5K and infrared observations will be made at wavelengths within the 5–200 $\mu$ m range. A coronagraphic instrument is currently being considered for the SPICA mission (Enya et al. 2006, Abe et al. 2006). The primary target of this instrument is the direct detection and observation of extra-solar Jovian outer planets (typically beyond 5AUs). The baseline requirements for the SPICA coronagraph are as follows: 10<sup>-6</sup> peak-to-peak contrast, smallest possible IWA, and a core wavelength within the range 5–20 $\mu$ m.

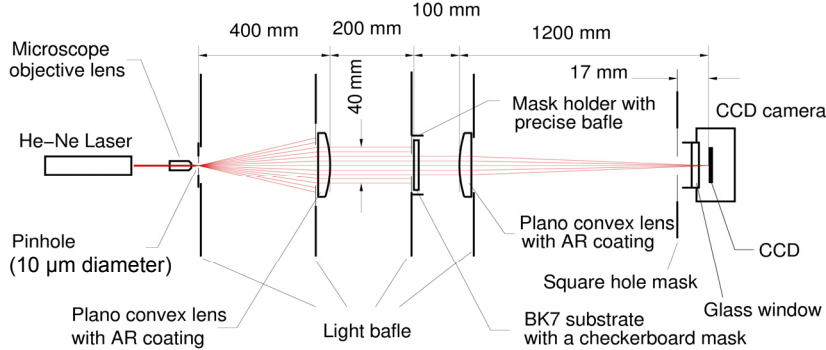
## LABORATORY EXPERIMENT

### Optical configuration

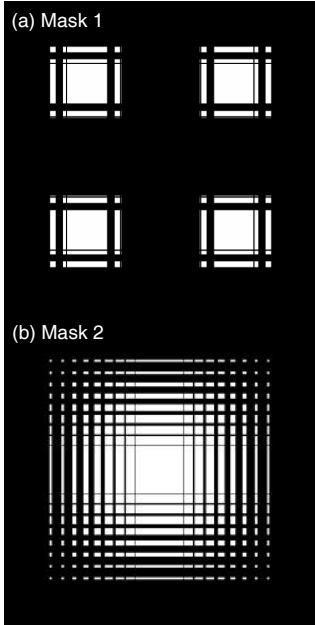
We chose to test 2 masks: one optimized for a pupil with a central obstruction and another for a clear pupil. In the optimized solutions providing throughput higher than 15%, the design which had the smallest IWA was adopted for manufacture. The targeted contrast to be demonstrated in this work was 10<sup>6</sup>, so that the mask was designed to achieve a contrast of 10<sup>7</sup>. The size chosen for the central obstruction of the first mask (Mask1, IWA of 7  $\lambda/D$ ) was 30% of the entrance pupil diameter. Subsequently, for comparison, a second mask (Mask2) was designed for a pupil without obstruction, and to probe the coronagraphic sensitivity at much lower IWA (3  $\lambda/D$ ). The OWAs for Masks1 and 2 were assumed to be 16 and 30  $\lambda/D$ . In our experiment,  $\lambda=632.8\text{nm}$  and  $D=2\text{mm}$  (i.e., the diagonal of our square masks). The smaller OWA gave a solution where the rectangular patterns of the mask were not too narrow and therefore made the fabrication simple and robust. The larger OWA provided a wider dark region while it made the fabrication more complex. Table 1 summarizes the specifications of the masks. Figure 2 shows the shape of the masks, and the expected coronagraphic point spread function (PSF) for Mask1 and Mask2.

Figure 1 shows a schematic of our optical setup. All the optics were set in a dark room with an air cleaning system. Clean air flowed from the top of the room to the optical table during the settings and measurements. Although we plan to use an adaptive optics system in future experiments, it was not used in this work. A He-Ne laser was used as the light source. A spatial filter consisting of a microscope objective lens and a 10 $\mu\text{m}$  diameter

pinhole was also used. A commercially available cooled CCD camera (BITRAN) with  $2048 \times 2048$  pixels was used to measure the PSF. The overall chip size was  $15.16\text{mm} \times 15.16\text{mm}$  with a flat glass window in front. The CCD was cooled and stabilized at  $0^\circ\text{C}$  throughout the experiment. The camera was mounted on a linear motor drive stage in order to scan along the optical axis to find the best focus position.



**Figure 1:** Laboratory experiment optical setup.



**Figure 2:** Mask1 and Mask2 theoretical shapes. Both masks are 2mm in diagonal.

## MASK FABRICATION

Each checkerboard mask consists of an aluminum film on a BK7 substrate, and were manufactured using nano-fabrication technology at the National Institute of Advanced Industrial Science and Technology (AIST) in Japan. A 100-nm thick film aluminum was evaporated onto the surface of the sub-strate. After evaporation, electron beam patterning and a lift-off process were applied to produce a rectangular trans-missive area for the checkerboard pattern. The substrate was 2mm thick and had no wedge angle. The flatness, parallelism and scratch-and-dig of the substrate were less than  $\lambda/10$ , 5 arcsecond and  $10^{-5}$  respectively. A narrow-band multiple-layer coating was applied to both sides of the substrate to reduce reflection at the surface after fabrication. The temper-ature of the mask during coating was kept less than  $100^\circ\text{C}$  to avoid deterioration of the residual resist around the mask pattern. The reduction in reflectivity of the BK7 substrate was confirmed to be less than 0.25% as a result of this coating. Small defects were found on Mask2, but we found no signi-ficant degradation in performance for this level of contrast.

## DATA ACQUISITION AND RESULTS

The dynamic range of the CCD was insufficient to capture the full dynamic range of the PSF in one single exposure. Therefore, several exposure times were used: 0.03, 0.1, 1.0, 10, 100, and 1800 seconds. The 1800 seconds exposure was for measurements in the dark region. The brightest region of the PSF saturated the detector even with the shortest exposure time, so we used additional neutral density filters with an optical density of 2. We also carefully checked the CCD linearity by imaging the PSF core through a combination of neutral density filters with a total optical density of 6, and with an 1800 seconds exposure. We found that no significant correction was needed so that we could rely on the multi-exposure time method.

The majority of the area of the dark region in the PSF with Mask1 is less than  $10^{-6}$  as shown in Figure3. On average, the observed contrast for each dark region on a linear scale is  $3.4 \times 10^{-7}$ ,  $2.1 \times 10^{-7}$ ,  $1.8 \times 10^{-7}$  and  $3.5 \times 10^{-7}$  for DR1, DR2, DR3 and DR4 respectively, where DR1–DR4 are the dark regions corresponding to the quadrants around the core shown in Figure4. The average contrast for all the dark regions is  $2.7 \times 10^{-7}$ . The  $3\sigma$  detection

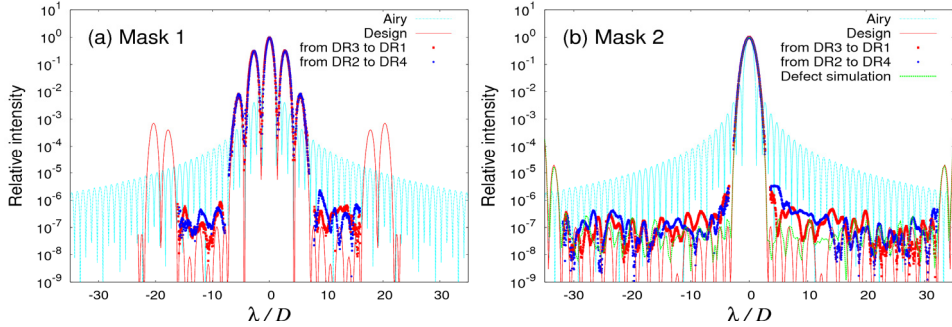


**Figure 3:** Diagonal cuts across PSFs of both Mask1 (left) and Mask2 (right).

limit computed within each observed dark region DR1–DR4 is  $7.5 \times 10^{-7}$ ,  $5.8 \times 10^{-7}$ ,  $4.1 \times 10^{-7}$ , and  $9.1 \times 10^{-7}$ , respectively. PSF subtraction or fitting has the potential to provide better performance, though such methods require assumptions about the repeatability of the pattern observed in the dark regions or the shape of the PSF. Therefore, the simple  $3\sigma$  limit corresponds to a conservative estimate of the detection limit. Nevertheless, all the values are below our  $10^{-6}$  limit.

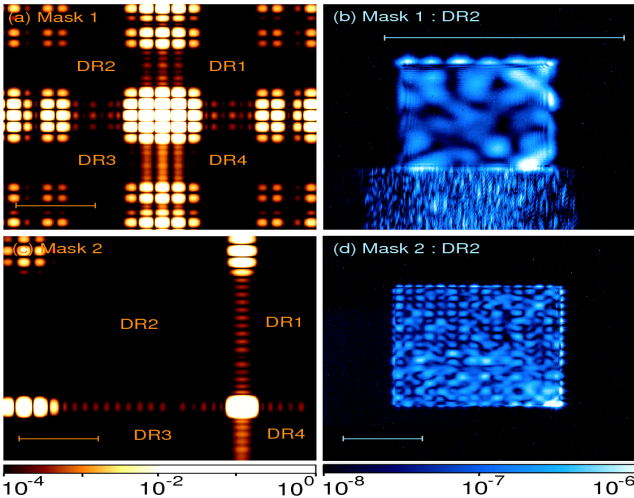


**Figure 4:** Mask1 and Mask2 PSFs (left) and close-up of the respective dark regions (right). The scale bar corresponds to  $10 \lambda/D$ .

using a binary checkerboard-type pupil shaped mask coronagraph. Although this kind of mask presents several limitations (large IWA and low throughput), its manufacture and implementation are very robust. Two masks, optimized for either obstructed pupil or not, were fabricated and tested. Both masks achieved a higher performance than the  $10^{-6}$  requirement:  $2.3 \times 10^{-7}$  and  $1.1 \times 10^{-7}$ . Therefore, we conclude that a binary checkerboard mask is a very attractive solution for the future MIR coronagraph of the SPICA space telescope, for which this study was carried out. Other coronagraphic solutions, more complex to implement are also considered, but the checkerboard mask can be regarded as the safest option.

**A more exhaustive description of this experiment is available at [astro-ph/0609646](#) (soon to appear in A&A).**

For the coronagraphic image with Mask2, the average contrast of DR1, DR2, DR3 and DR4 on a linear scale is  $1.1 \times 10^{-7}$ ,  $1.0 \times 10^{-7}$ ,  $9.0 \times 10^{-7}$  and  $1.3 \times 10^{-7}$ , respectively. The average contrast of the whole dark region is  $1.1 \times 10^{-7}$ . The  $3\sigma$  limit is  $3.8 \times 10^{-7}$ ,  $3.0 \times 10^{-7}$ ,  $2.7 \times 10^{-7}$  and  $3.8 \times 10^{-7}$  for DR1, DR2, DR3 and DR4 respectively. In the bottom part of Figure 4(d), an irregular speckle pattern can be observed, getting brighter close to the optical axis (bottom right). This pattern was invariant in repeated measurements with a fixed setup. Change in the air flow and suspension conditions made no significant difference in the observed image. On the contrary, when we shifted and rotated the mask, this speckle pattern changed, suggesting the same limiting factors as for Mask1.

## CONCLUSION

We reported the results from a laboratory experiment using a binary checkerboard-type pupil shaped mask coronagraph. Although this kind of mask presents several limitations (large IWA and low throughput), its manufacture and implementation are very robust. Two masks, optimized for either obstructed pupil or not, were fabricated and tested. Both masks achieved a higher performance than the  $10^{-6}$  requirement:  $2.3 \times 10^{-7}$  and  $1.1 \times 10^{-7}$ . Therefore, we conclude that a binary checkerboard mask is a very attractive solution for the future MIR coronagraph of the SPICA space telescope, for which this study was carried out. Other coronagraphic solutions, more complex to implement are also considered, but the checkerboard mask can be regarded as the safest option.

## REFERENCES

- Abe, L. et al., 2005, proc. of IAU Colloquium **200**, 329
- Enya, K. et al. 2006, proc. of SPIE, **6265**, 97
- Kasdin, N. J. et al., 2003, ApJ, **582**, 1147
- Nakagawa, T. and SPICA working group, 2004, Adv. Sp. Res., **34**, 645